

Electron-impact ionization cross sections out of the ground and 6^2P excited states of cesium

M. Łukomski,^{1,2} S. Sutton,¹ W. Kedzierski,¹ T. J. Reddish,^{1,*} K. Bartschat,³ P. L. Bartlett,⁴ I. Bray,⁴
A. T. Stelbovics,⁴ and J. W. McConkey^{1,5,†}

¹*Department of Physics, University of Windsor, Ontario, Canada N9B 3P4*

²*Instytut Fizyki, Uniwersytet Jagielloński, ul. Reymonta 4, 30-059 Kraków, Poland*

³*Department of Physics, Drake University, Des Moines, Iowa 50311, USA*

⁴*The ARC Centre for Antimatter-Matter Studies, Murdoch University, Perth, Australia*

⁵*Jet Propulsion Laboratory, California Institute of Technology, 6800 Oak Grove Dr., Pasadena, California 91109, USA*
(Received 1 November 2005; revised manuscript received 21 February 2006; published 21 September 2006)

An atom trapping technique for determining absolute, total ionization cross sections (TICS) out of an excited atom is presented. The unique feature of our method is in utilizing Doppler cooling of neutral atoms to determine ionization cross sections. This fluorescence-monitoring experiment, which is a variant of the “trap loss” technique, has enabled us to obtain the experimental electron impact ionization cross sections out of the Cs $6^2P_{3/2}$ state between 7 eV and 400 eV. CCC, RMPS, and Born theoretical results are also presented for both the ground and excited states of cesium and rubidium. In the low energy region (<11 eV) where best agreement between these excited state measurements and theory might be expected, a discrepancy of approximately a factor of five is observed. Above this energy there are significant contributions to the TICS from both autoionization and multiple ionization.

DOI: [10.1103/PhysRevA.74.032708](https://doi.org/10.1103/PhysRevA.74.032708)

PACS number(s): 34.80.Dp, 32.80.Pj

I. INTRODUCTION

Collisions between electrons and excited atomic species are important wherever electrical discharges or plasmas are encountered. However obtaining quantitative cross section data for such processes has proved to be extremely difficult and so relatively few such data sets have been reported [1]. In the last decade there has been a growth in the use of magneto-optical traps (MOTs) in conjunction with electron impact techniques, resulting in measurements of total electron scattering cross sections [2–5] and ionization cross sections [6,7]. In this work we report the first measurements and calculations of the electron-impact *total* ionization cross section (TICS) from the excited $6^2P_{3/2}$ state of cesium. Not only are such TICSs from short-lived states of great practical relevance in plasmas and discharges [1,8], they are important also for developing a theoretical understanding of ionization processes in large multielectron systems.

The technical difficulties in measuring absolute cross sections from excited states are well known. This is further compounded if the target is a metal vapor, as in the present study, due to the inherent low number density in the interaction region. That there have been no *ground* state electron impact ionization cross section measurements since the 1960s [9–14] is perhaps indicative of the technical limitations in using conventional methods. Some of those experimental challenges can, however, be overcome using atom trapping techniques.

In our earlier electron-impact studies using a MOT, we used the “trap loss” method to measure the ground state total

scattering cross sections in cesium [3,5]. The trap-loss technique, first developed by Lin and co-workers [2,6,7], monitors the fluorescence decays of the trapped atoms, with and without an electron beam present. The loss rate of atoms from the trap due to electron collisions, Γ_e , is related directly to the cross section, σ , and electron flux, J , through the trap

$$\Gamma_e = \sigma J l e. \quad (1)$$

Hence measurements of Γ_e and J yield σ directly. In this work, we still monitor the trap fluorescence, however, altering the timing sequence for the pulsed magnetic field and electron beam, together with the trapping and repumping lasers, we have been able to determine the loss of atoms from the trap due solely to ionization. We take full advantage of the fact that (a) it is not necessary to know the target density using the trap loss method, (b) laser pumping allows one to create a known, substantial fraction of atoms in a specific state, and (c) in the present experiment Doppler cooling only acts on neutral atoms, allowing the ions to escape the interaction region.

II. EXPERIMENTAL METHOD

Experimental details of our MOT system are available elsewhere [3,5]; only information pertinent to this ionization study is presented here. Cesium is introduced into the UHV vacuum chamber via a valved side-arm reservoir maintained at a constant temperature and the trap is reloaded from the background Cs vapor. The internal anti-Helmholtz pair of coils providing the magnetic trapping field has an axial field gradient of approximately 10 G/cm for an operating current of 2 A. The pulsing on and off of the coil current is controlled via a TTL signal and the circuit also provides a means of rapidly switching the coil current to minimize the magnetic field rise and decay times (<1 msec). Laser cooling of

*Author to whom correspondence should be addressed. Electronic address: reddish@uwindsor.ca

†Author to whom correspondence should be addressed. Electronic address: mcconk@uwindsor.ca

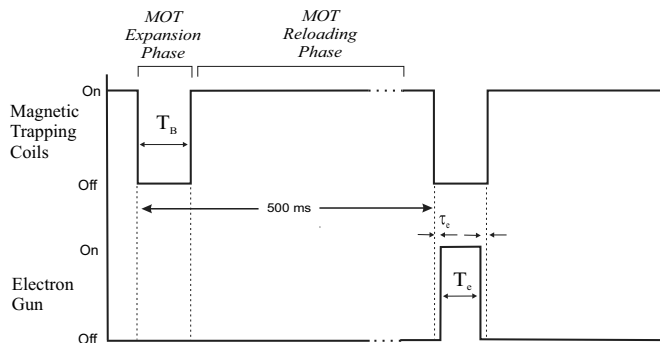


FIG. 1. Timing sequence diagram for this experiment: $T_B = 10$ ms, $T_e = 8$ ms, and $\tau_c = 1$ ms. The electron beam is present for alternate measurement cycles.

the Cs atoms is achieved with two external cavity, grating stabilized diode lasers operating at 852 nm. The trapping laser is red detuned from the $6^2S_{1/2}(F=4) \rightarrow 6^2P_{3/2}(F=5)$ transition frequency. The repumping laser is set to the $6^2S_{1/2}(F=3) \rightarrow 6^2P_{3/2}(F=4)$ transition to remove atoms from the dark ($F=3$) ground state. The merged trapping and repumping laser beams have ~ 17 mm diameter in the vacuum chamber. The trapped atom fluorescence is collected and monitored continuously using a cooled photomultiplier tube.

A multielement electron gun produces a near parallel 10 mm diameter beam of uniform current density over the entire 7–400 eV energy range covered in this study [5]. An oxide coated cathode is used and two pairs of electrostatic deflectors allow accurate control and steering of the ~ 70 μ A electron beam. Two movable wire probes are arranged so that the electron beam profile can be monitored in two dimensions in a plane perpendicular to the electron beam direction. The current density, J , in the region of the atom cloud is obtained from measurements of the electron beam profile and the total beam current collected in the Faraday cup. Helium was introduced into the vacuum system to calibrate the energy scale using the He^+ threshold at 24.58 eV in a time-of-flight ion detection system. The error in the energy calibration is estimated to be ± 0.3 eV.

During the experiment, the trapping magnetic field was turned off for a time, T_B , (10 ms), as shown in the timing sequence diagram of Fig. 1. During alternate trap-off times an electron beam pulse was introduced for a time, T_e (8 ms), after a delay of τ_c (1 ms) to ensure that the electrons were not perturbed during the magnetic field switching. Trap fluorescence was monitored continuously with the signals from alternate cycles, each lasting 500 ms, being stored in separate memories. The Faraday cup current was also continuously monitored. Further measurements, taken with the trapping magnetic field permanently off, were obtained in order to subtract the corresponding background fluorescence due to untrapped atoms or scattered laser light. The time evolution of the trap fluorescence, both with and without the presence of the electron beam pulse, is shown in Fig. 2.

In the current experiment both the trapping and repumping lasers were permanently on. The cesium ions produced by electron impact are not slowed down by this laser field.

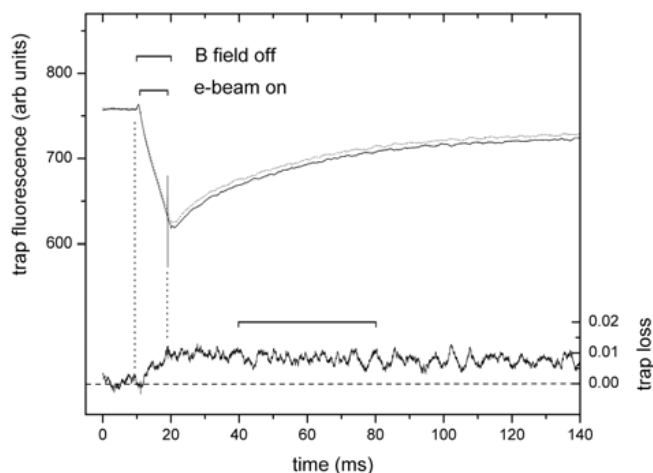


FIG. 2. *Upper traces*: Typical trap fluorescence curves, after background subtraction, with (solid) and without (dashed) the electron beam present. The losses in the absence of the electron beam are due to a variety of factors, including thermal expansion and collisions within the trap and with vacuum residuals. Of relevance are the *additional* losses due to the presence of the electron beam. *Lower Trace*: The trap loss as a function of time derived from the upper two traces as discussed in [5]. The horizontal bar indicates the time interval used to determine the average trap loss rate, Γ_e , in this work.

However, Doppler cooling of the (neutral) atoms is continually present and this inhibits the atoms which gain momentum via electron collisions from escaping the interaction region. Even so, the fastest recoiling atoms in the trap can escape the interaction region even when trapping and repumping lasers are on, which could potentially result in an overestimation of the measured TICS. To evaluate the significance of the trap loss contribution due to nonionizing electron collisions we obtained TICS measurements as a function of time T_B , for fixed values of T_e and τ_c . Recoil velocity increases with increasing electron scattering angle and large-angle scattering is more prominent at low electron impact energies. However, low energy electrons have less momentum to impart so it is necessary to examine these counteracting effects at both low and high electron impact energies. Similar tests were performed by Schappe *et al.* [6], who found the low energy Rb TICS measurements to be more sensitive to this loss mechanism. The data in Fig. 3 show that the deviations of our TICS values, as a function of time when the trapping force is absent, are small compared to our experimental uncertainty. This indicates that the laser beams are very effective in slowing down those atoms that gain momentum during electron collisions. We can therefore assume that losses measured during the experiment are overwhelmingly due to the production of ions. The use of Doppler cooling to stop atoms from escaping the interaction region is a novel feature of this electron impact MOT technique.

A further result of both trapping and repumping lasers being present during the electron-atom interaction is that the atoms in the trap are in a mixture of $6^2S_{1/2}$ and $6^2P_{3/2}$ states.

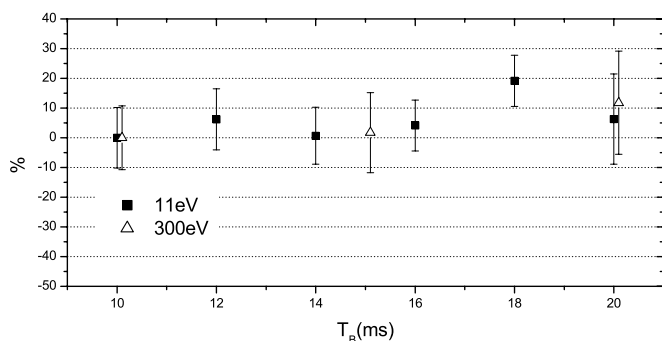


FIG. 3. Graphs showing the percentage deviations in the measured TICS values as a function of T_B for two electron beam energies. Doubling T_B does not alter the TICS values (within experimental uncertainty), indicating that laser cooling effectively inhibits scattered atoms from escaping the trap region.

Following Keeler *et al.* [7], the excited state fraction, f_e , can be estimated using the following two level atom approximation

$$f_e = \frac{I/2I_s}{1 + I/I_s + 4\Delta^2/\Gamma^2} \quad (2)$$

where Δ is the detuning of the trapping laser from resonance, I is the applied laser intensity at the trap, I_s is the saturation intensity, and Γ is the natural linewidth of the trapping transition (32.7686 MHz). The two-level approximation is reasonable here given the fact that further excitation or ionization from the excited level is not energetically feasible using single 852 nm photons. Measurements of trap fluorescence as a function of laser intensity with constant $\Delta=19$ MHz resulted in evaluation of the excited state fraction in the cold Cs atom cloud. For these measurements we used a Pockels cell to rapidly rotate the polarization of the trapping laser beam to control the intensity while maintaining a constant number of atoms in the trap. From this method we estimate the trap to contain $26(\pm 1)\%$ of excited $6^2P_{3/2}$ state cesium, with the remaining 74% in the $6^2S_{1/2}$ ground state. We note that our excited state fraction is similar to that obtained by other workers using similar traps: e.g., Keeler *et al.* [7] (43%). The total ionization cross section measurements presented later in Fig. 6 were evaluated from raw data obtained with this state mixture. Typical TICS uncertainties ($\Delta\sigma$) are $\sim 11\%$, largely due to the statistical fluctuations in the measured loss rates (see [5] for further discussion).

III. THEORETICAL APPROACHES

We utilize three theoretical approaches for estimating the Cs electron-impact ionization cross sections. The nonperturbative convergent close coupling (CCC) [15] and the R matrix with pseudostates (RMPS) [16] methods are supplemented by a Born based approach [17]. Whereas the former two yield cross sections for ejecting only the valence electron, the latter is also able to estimate the cross section for ejecting a core electron.

The first step in a collision calculation is to have an adequate description of the target. For the alkali metals this has been studied in some detail and basically the same approach is adopted here by all three calculations. The core orbitals are obtained from a self-consistent-field Hartree-Fock treatment of the ground state of Cs. These core orbitals are then used to define the frozen-core Hartree-Fock or an equivalent local core potential, which is supplemented by an appropriately chosen core-polarization potential. The full core potential is checked by ensuring, upon solution of the Schrödinger equation, the resulting valence electron energies and oscillator strengths are in good agreement with experimental values.

Unlike the common approach to structure, the three methods differ substantially in their approach to the scattering part of the calculation. While both the RMPS and CCC methods are based on the close-coupling approach, with the target continuum modeled with the usage of pseudostates, their numerical implementation is very different. The RMPS method obtains the target states by diagonalizing the target Hamiltonian using a Slater-type representation and solves the full problem of projectile plus target atom in a box to yield results over a fine, but not too broad an energy range. On the other hand, in the CCC method the target states are obtained by diagonalizing the target Hamiltonian in a Laguerre basis, and the method is applied separately at any energy of interest by solving the coupled equations in momentum space.

The Born calculations presented here are based on the analytic Born approximation technique described in [17] and target wave functions calculated using the Hartree-Fock (HF) self-consistent field technique. We used the computer program described in [18] to generate the HF wave functions with a Slater basis, and included an estimate for core polarization for the valence orbital calculations. The same core orbitals were used for both ground-state and excited-state calculations. The Born method [17] uses a plane wave to model the scattered electron and a Coulomb wave for the ejected electron, which is orthogonalized to the occupied orbitals of the target. Moreover, we progressively orthogonalized to the nearest unoccupied orbitals until convergence was obtained. This was achieved by including the first two unoccupied orbitals ($5p$ and $6s$ for Rb 5^2S ; $5s$ and $6s$ for Rb 5^2P ; $6p$ and $7s$ for Cs 6^2S ; $6s$ and $7s$ for Cs 6^2P) in the orthogonalization of the Coulomb wave. This extended orthogonalization had a minimal effect on the core or excited-state cross sections, but some effect on the ground-state ionization at the higher energies. Despite the rather different numerical approaches, we shall see that the three calculations yield very similar cross sections for ejecting the Cs $6s$ or $6p$ electron by electron-impact at all energies considered here.

IV. RESULTS AND DISCUSSION

To extract the Cs 6^2P TICS, it is necessary to have an accurate and reliable $6^2S_{1/2}$ TICS in order to subtract its contribution from the measured total ionization yield. Although the measurements of Nygaard [14] and Zapesochnyĭ and Aleksakhin [12] are in good agreement, the data of Korchevoĭ and Przonski [11] and Heil and Scott [10] are, respectively, ~ 1.2 and ~ 0.65 that of Nygaard's results in the

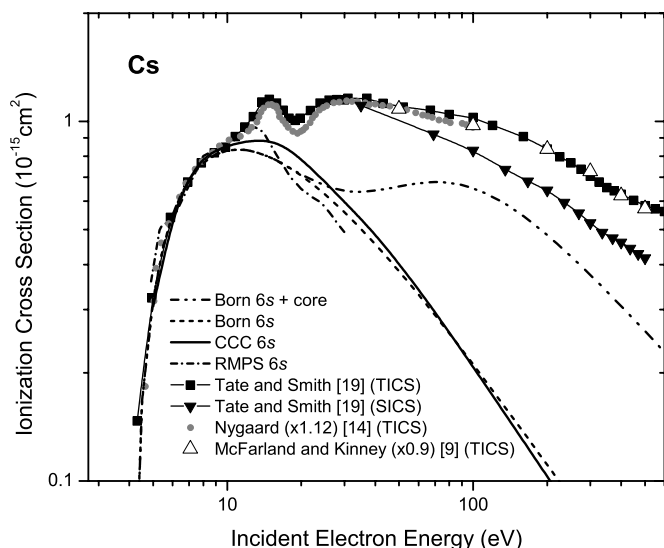


FIG. 4. Experimental TICS from the Cs ground state, rescaled to CCC and RMPS calculated SICS between 4–10 eV, as discussed in the text. The Born SICS also show the contribution from 5*p* and 5*s* core ionization, with calculated threshold energies of 22.9 and 38.0 eV, respectively. Tate and Smith’s [19] rescaled SICS is also shown, indicating the contribution to the TICS from multiple ionization.

region of overlap below 25 eV. In this work we present theoretical *single* ionization cross sections (SICS), shown in Fig. 4, obtained using the CCC, *R* matrix with pseudostates (RMPS), and Born approximation methods. Both the CCC and RMPS calculations only consider direct single ionization from either the 6*s* or 6*p* orbitals. The Born calculations include single ionization from the 5*p* and 5*s* core orbitals, which accounts for a prominent shoulder in the SICS at ~100 eV. None of these theoretical methods account for autoionization (or multiple ionization). Although there are small differences in the CCC, RMPS, and Born shapes above 12.3 eV, the onset of the lowest autoionizing state, there is excellent agreement in their magnitudes up to ~10 eV. Consequently, we have renormalized Nygaard’s data [14] to our calculations in the region between 4–10 eV using a scaling factor of 1.12. McFarland and Kinney’s TICS data [9] were then scaled by 0.9 to merge with the scaled Nygaard results in the 50–100 eV region of overlap (see Fig. 4). The relative TICS data of Tate and Smith [19] were also normalized to the CCC and RMPS results in the 4–10 eV region. The result of this renormalization is excellent agreement in the shape of the experimental TICS over the entire 4.5–800 eV region, affirming Tate and Smith’s pioneering results. It should be noted that Nygaard [14], McFarland and Kinney [9] and Zapesochnyĭ and Aleksakhin [12] estimate their experimental uncertainties to be ±7%, ±10%, ±15%, respectively. Thus applying our scaling factors is not unreasonable.

Having established a reliable 6²*S*_{1/2} TICS and the fraction of excited state Cs in the trap, we are able to determine the TICS (6²*P*)/TICS(6²*S*) ratio, as well as the electron impact TICS from the 6²*P*_{3/2} state. We emphasize that this is done by subtracting the *experimental* 6²*S*_{1/2} TICS from the total

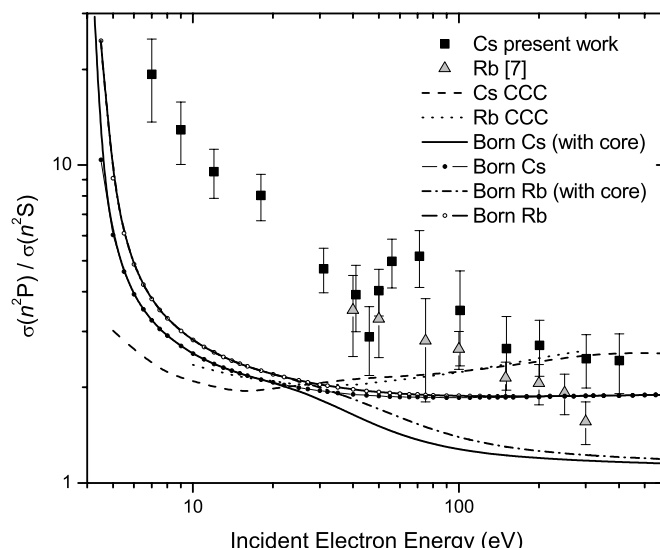


FIG. 5. The ratios of the ²*P*/²*S* ionization cross sections from rubidium and cesium, as discussed in the text. Thresholds for Cs^{*n*+} for *n*=1 to 3 are 3.89, 27.05 eV, and 62 eV, respectively, from the ground state configuration. The corresponding Rb²⁺ threshold lies at 31.47 eV.

TICS for all energies considered. The RMPS and CCC theories, below the onset of autoionization and core ionization around 12 eV, are *only* used to establish the overall normalization of these experimental cross sections. The results are shown in Figs. 5 and 6, respectively. Note that the error bars in both figures do not include the uncertainties associated with the ground state TICS. The Cs TICS (6²*P*)/TICS(6²*S*) ratio in Fig. 5 is also compared to the corresponding experimental SICS (5²*P*)/SICS(5²*S*) ratio in Rb [7]. The Rb and Cs ratios are remarkably similar at the lowest energies (40–50 eV) of available Rb data, and despite overlapping error bars above 100 eV, the overall trend is for slightly

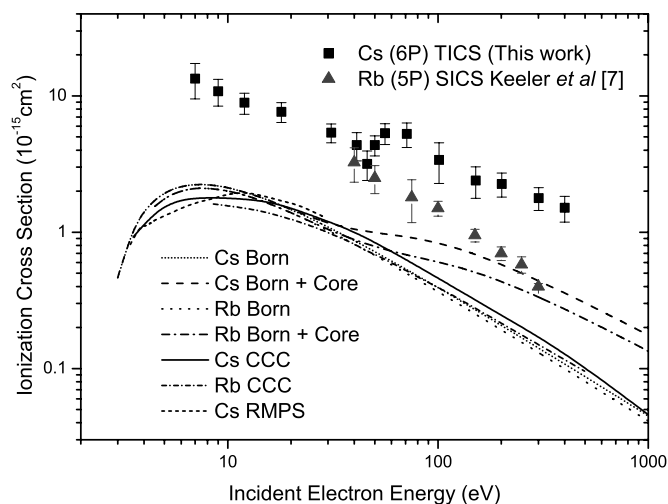


FIG. 6. The measured TICS out of the Cs 6²*P*_{3/2} state compared to SICS from CCC, RMPS and Born calculations. For comparison, the results of our CCC, and Born SICS calculations for Rb 5²*P* state are also compared to the SICS data of Keeler *et al.* [7].

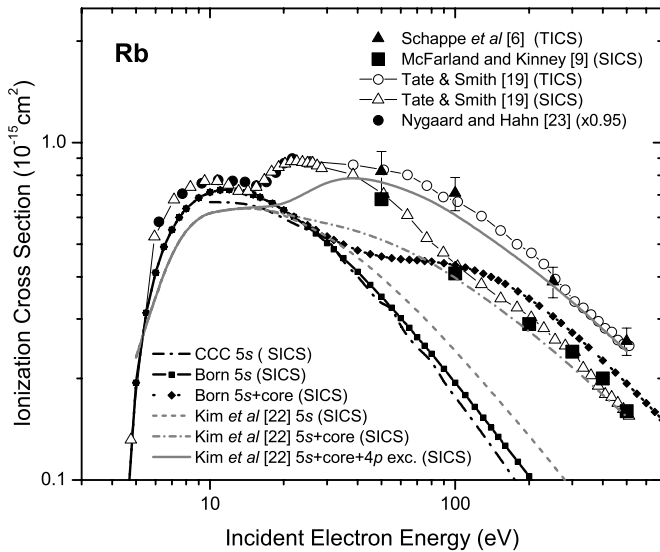


FIG. 7. Summary of the theoretical and experimental status for ground state ionization of rubidium.

lower Rb ratios. We note that the Rb data only correspond to *single* ionization and were obtained using very different detection techniques from that of this study. The CCC and Born SICS ratios for Rb are also shown, and are remarkably similar to their corresponding ratios for Cs at all energies.

Both Figs. 5 and 6 feature a small relative increase in the measured Cs ionization yield beginning at ~ 50 eV from the otherwise monotonically decreasing cross section/ratio. Our Born calculations for Cs use the same core orbitals; hence the inclusion of core ionization necessarily reduces the ratio towards unity and cannot account for the observed ratio *increase*, despite the similarity in threshold energies. The thresholds for Cs^{2+} and Cs^{3+} , whose cross section maxima occur at about 100 eV and 130 eV, respectively, also occur in this energy region and their contribution to the TICS is estimated to be $\sim 17\%$ at ~ 75 eV [19,9] (see Fig. 4). Quantitatively, McFarland [13] finds the peak σ^{++} magnitude to be essentially the same for both Cs and Rb, namely $\sim 1.2 \times 10^{-16} \text{ cm}^2$ at ~ 100 eV. We note too that prominent broad peaks in the electron impact autoionization cross sections occur in precisely the same energy region [20,21] and cannot be neglected. Nevertheless, given the experimental comparison with Rb SICS data, the observed ratio increase in Fig. 5 is most likely due to relative differences in the coupling of the multiple ionization channels to the Cs ground $6^2S_{1/2}$ and $6^2P_{3/2}$ excited states.

Before discussing the excited state ionization cross sections shown in Fig. 6, attention is drawn to the Rb ground state ionization cross sections presented in Fig. 7. This figure compares previously published experimental data to our CCC and Born SICS results, together with those of Kim *et al.*'s binary-encounter-dipole (BED) model [22]. The following points should be noted. First, the SICS value of McFarland and Kinney [9] at 50 eV was used to normalize Tate and Smith's relative SICS [19], which then show excellent *shape* agreement at higher energies. This also calibrates Tate and Smith's TICS, which are then in excellent accord with the more recent TICS of Schappe *et al.* [6]. Second, Nygaard

and Hahn's [23] Rb data are not included at energies above the threshold for multiple ionization, 31.5 eV, as they present $\Sigma n\sigma^{n+}$ rather than $\Sigma\sigma^{n+}$ [24]. The data below ~ 25 eV of Nygaard and Hahn [23] were simply scaled by 0.95, to show that its shape agrees with that of Tate and Smith. Although the experimental results are higher than new CCC results by $\sim 10\%$ at 10 eV, this is within Tate and Smith's experimental uncertainty. Third, we note that CCC and Born are in very good agreement for 5s ionization. Kim *et al.*'s [22] 5s results are systematically larger than CCC and Born at higher energies. Fourth, we note that, as in the case of cesium (see Fig. 4), the contributions of autoionization, core, and multiple ionization are a significant part of the TICS for Rb. This is highlighted by Kim *et al.*'s [22] SICS results, which incorporate both core and autoionization (primarily from 4p excitation). These contributions could be overestimated, as the overall result seems to agree better with the experimental TICS, rather than SICS. They anticipate that this latter contribution may be an overestimate, as they used the Born method to treat autoionization. Our Born results also appear to overestimate the core ionization contribution, as the resultant Rb SICS are larger than the experimental SICS.

The Cs and Rb ground state ionization results of Figs. 4 and 7, respectively, are significantly different from the excited state results of Fig. 6. First, one notes the remarkable similarity in the shapes and magnitudes in the theoretical cross sections for the two targets. This suggests that we may make a direct comparison of the experimental data. Second, at ~ 50 eV, where the Rb and Cs experimental data overlap, their cross sections are ~ 3.5 times larger than the CCC results. This is larger than in the ground state scenarios for both targets, where the corresponding factor is ~ 2 . Furthermore, since the experimental Cs and Rb data correspond to TICS and SICS, respectively, the observed difference above 50 eV is, presumably, mainly due to multiple ionization contributions, as in Fig. 5. This is plausible as the relative contribution of multiple ionization to the TICS appears similar to that observed in ground state Cs and Rb (see Figs. 4 and 7).

We cannot account for the large discrepancy between theory and experiment below the autoionization onset at ~ 11 eV; i.e., the energy region where comparison is justifiable. We are not aware of any inherent energy-dependent systematic error in the experiment; the same apparatus was used in ground state total electron impact cross section measurements covering a similar energy range which show very good agreement with other available experimental and theoretical results [5].

The discrepancy in excited state ionization cross section magnitudes between experiment and best available theory is disturbing but not unique to Cs and Rb. For example, we note that experimental electron impact TICS from metastable 2^3S He [25] are about a factor 2 higher than state-of-the-art RMPS [26] and CCC calculations [27].

V. CONCLUSION

Both theory and experiment, despite the lack of convergence, provide important information pertaining to the ex-

cited state ionization cross sections of heavy alkali metals. Autoionization and multiple ionization processes are shown to make significant contributions to the ground state TICS. Consequently these mechanisms need to be incorporated into future excited state calculations to enable a legitimate comparison with experiment.

ACKNOWLEDGMENTS

This work was supported, in part, by ARC (Australia), NSF (USA) [under PHY-0244470 (K.B.)], and by the Canadian agencies CIPI, CFI, OIT, and NSERC. I.B. is grateful to ISA Technologies, Perth, Western Australia for access to their IBM P690 computer.

-
- [1] L. G. Christophorou and J. K. Olthoff, *Adv. At., Mol., Opt. Phys.* **44**, 155 (2001).
- [2] R. S. Schappe, P. Feng, L. W. Anderson, C. C. Lin, and T. Walker, *Europhys. Lett.* **29**, 439 (1995).
- [3] J. A. MacAskill, W. Kedzierski, J. W. McConkey, J. Domysławska, and I. Bray, *J. Electron Spectrosc. Relat. Phenom.* **123**, 173 (2002).
- [4] L. J. Uhlmann, R. G. Dall, A. G. Truscott, M. D. Hoogerland, K. G. H. Baldwin, and S. Buckman, *Phys. Rev. Lett.* **94**, 173201 (2005).
- [5] M. Łukowski, J. A. MacAskill, D. P. Seccombe, C. McGrath, S. Sutton, J. Teeuwen, W. Kedzierski, T. J. Reddish, J. W. McConkey, and W. A. van Wijngaarden, *J. Phys. B* **38**, 3535 (2005).
- [6] R. S. Schappe, T. Walker, L. W. Anderson, and C. C. Lin, *Phys. Rev. Lett.* **76**, 4328 (1996).
- [7] M. L. Keller, L. W. Anderson and C. C. Lin, *Phys. Rev. Lett.* **85**, 3353 (2000).
- [8] H. Deutsch, P. Scheier, S. Matt-Luebner, K. Becker, and T. D. Märk, *Int. J. Mass. Spectrom.* **243**, 215 (2005).
- [9] R. H. McFarland and J. D. Kinney, *Phys. Rev.* **137**, A1058 (1965).
- [10] H. Heil and B. Scott, *Phys. Rev.* **145**, 279 (1966).
- [11] Y. P. Korchevoĭ and A. M. Przonski, *Sov. Phys. JETP* **24**, 1089 (1967).
- [12] I. P. Zapesochnyĭ and I. S. Aleksakhin, *Sov. Phys. JETP* **28**, 41 (1967).
- [13] R. H. McFarland, *Phys. Rev.* **159**, 20 (1967).
- [14] K. J. Nygaard, *J. Chem. Phys.* **49**, 1995 (1968).
- [15] I. Bray, D. V. Fursa, A. S. Kheifets, and A. T. Stelbovics, *J. Phys. B* **35**, R117 (2002).
- [16] K. Bartschat and Y. Fang, *Phys. Rev. A* **62**, 052719 (2000).
- [17] P. L. Bartlett and A. T. Stelbovics, *Phys. Rev. A* **66**, 012707 (2002); *At. Data Nucl. Data Tables* **86**, 235 (2004).
- [18] J. Mitroy, *Aust. J. Phys.* **52**, 973 (1999).
- [19] J. T. Tate and P. T. Smith, *Phys. Rev.* **46**, 773 (1934).
- [20] V. Pejčev and K. J. Ross, *J. Phys. B* **10**, L291 (1977).
- [21] S. Kaur and R. Srivastava, *J. Phys. B* **32**, 2323 (1999).
- [22] Y-K. Kim, J. Migdalek, W. Siegel, and J. Bieroń, *Phys. Rev. A* **57**, 246 (1998).
- [23] K. J. Nygaard and Y. B. Hahn, *J. Chem. Phys.* **58**, 3493 (1973).
- [24] The same is most probably true for the McFarland and Kinney data cited in L. J. Kieffer and G. H. Dunn, *Rev. Mod. Phys.* **38**, 1 (1966).
- [25] A. J. Dixon, M. F. A. Harrison, and A. C. H. Smith, *J. Phys. B* **9**, 2617 (1976).
- [26] K. Bartschat, *J. Phys. B* **35**, L527 (2002).
- [27] D. V. Fursa and I. Bray, *J. Phys. B* **36**, 1663 (2003).